

Purification of superposed coherent states via partial homodyne detection

Shigenari Suzuki,^{1,2} Masahiro Takeoka,^{1,3} Masahide Sasaki,^{1,3} Ulrik L. Andersen,⁴ and Fumihiko Kannari²

¹*Quantum Information Technology Group, National Institute of Information and Communications Technology (NICT),
4-2-1 Nukui-kitamachi, Koganei, Tokyo 184-8795, Japan*

²*Department of Electronics and Electrical Engineering, Keio University,
3-14-1, Hiyoshi, Kohoku-ku, Yokohama, 223-8522, Japan*

³*CREST, Japan Science and Technology Agency, 1-9-9 Yaesu, Chuoh-ku, Tokyo 103-0028, Japan*

⁴*Institut für Optik, Information und Photonik, Max-Planck Forschungsgruppe,
Universität Erlangen-Nürnberg, Günther-Scharowsky str. 1, 91058, Erlangen, Germany*

We present a simple protocol to purify a coherent state superposition from a statistical mixture of a superposed states and coherent states. The scheme constitutes only a single beam splitter and a homodyne detector, and thus experimentally feasible. In practice, a superposition of coherent states is transformed into such a mixture by linear loss, which is usually the dominant decoherence mechanism in optical systems. We also address the possibility of producing a larger amplitude superposition state from decohered states, and show that in most cases the decoherence of the states are amplified along with the amplitude.

PACS numbers: 03.67.Hk, 42.50.Dv

I. INTRODUCTION

In optical communication systems, information is often carried by states with Gaussian statistics; the coherent state is a simple and very important example. The processing of these states in the quantum domain is now a major concern toward attaining ultimate capacity of bosonic channels [1, 2], and also the construction of quantum networks and computers [3, 4]. To enable an arbitrary processor, that is to develop the full set of gates allowing for universal quantum operations, one needs any required order of optical nonlinear interactions between Gaussian states. It has been shown that any cubic or higher order Hamiltonian in terms of the annihilation and creation operators $\{\hat{a}, \hat{a}^\dagger\}$ in cascade of linear and bilinear order Hamiltonians suffices for the implementation of arbitrary multi-mode Hamiltonians, which in turn permits the construction of an arbitrary gate [5]. The linear and bilinear order Hamiltonians can be generated using linear optics and squeezing operations, respectively, and thus feasible with current technology. As for the cubic order Hamiltonians, it has been shown recently that the cubic phase gate $\hat{V}_\gamma = \exp(i\gamma\hat{x}^3)$, where \hat{x} is the quadrature amplitude operator and the real number γ represents the amount of nonlinear phase shift, can be executed by interacting the signal with a non-Gaussian ancillary state assisted by a bilinear order Hamiltonian. This ancilla, called the cubic phase state, can be generated by squeezing one half of an Einstein-Podolsky-Rosen (EPR) state, with the degree of squeezing being conditioned on the number of photons in a displaced version of the other half of the EPR state [6, 7, 8]. This kind of nonlinear ancillary state is often given by a macroscopic or mesoscopic superposition of distinct wave functions and, toward the realization of universal operations, it is of high importance to investigate the preparation of such states under realistic conditions.

A simple example and presently more experimentally

feasible example is the generation of a quantum superposition of coherent states with small amplitudes. Such a state can be conditionally generated by using the photon number measurement [9], much like the generation of the above mentioned cubic phase state. A proof-of-principle experiment of this idea was recently presented in ref [10], where an on/off-type detector (which clicks upon the arrival of a photon) was used rather than a photon number resolving detector. Such a superposition state can be equivalently generated by squeezing a single photon state. Furthermore, it has recently been shown that the amplitudes of the constituents of the superposition state can be amplified using linear optics and on/off detectors [11, 12]. However, it is well known that such macroscopic superposition states are easily destroyed by losses and, in practice, the states prepared in labs are usually imperfect statistically mixed states. Therefore, there is a need for a purification scheme, that transforms the statistical mixed state into a pure state.

In this paper, we develop a feasible scheme to purify coherent superposition states that has undergone linear dissipation. The scheme is based only on the use of a single beam splitter and a single homodyne detector, which probabilistically selects out favourable events. To simplify the problem, we consider a simple superposition of two distinct coherent states. In the presence of linear loss, such coherent superposition state (CSS) transforms into a mixture of a CSS and a statistically mixed coherent state. Our task is then to reduce the probability of the mixed coherent state component, and hereby recover the CSS as efficiently as possible.

The CSS itself has also been discussed as a resource of various optical quantum information processing protocols [13, 14, 15, 16, 17, 18, 19, 20] and, as a related topic to our study, Glancy *et al.* have proposed a method to restore a CSS in which one-qubit information is encoded, by applying a three-bit quantum error correcting code [21]. However, this proposal requires almost perfect

photon number resolving detectors and, moreover, pure CSSs as ancillary states. In our study we make no use of non-Gaussian ancillary states.

The schematic of our proposal is shown in Fig. 1. A fraction of the input state is tapped off by a beam splitter and subsequently measured with a homodyne detector. From the measurement outcomes we try to distinguish the CSS from the mixture of coherent states through the differences of their wave functions. Based on the success of this estimation, the coherence of the CSS is retrieved through selection of favourable events. In the paper we show that homodyne measurement is one of the optimal measurements providing the most efficient purification given such a simple setup.

Using the purification protocol in Fig. 1, inevitably the amplitude of the coherent state components in the CCS is degraded due to the partial measurement strategy. Therefore we also address the possibility to recover the amplitude by using the CSS amplification scheme proposed in Refs [11, 12].

This paper is organized as follows. In section II, the influence of linear dissipation to the CSS is briefly reviewed. In section III, we discuss the purification scheme in general terms without specifying the exact measurement strategy applied to the tapped off state. In section IV, we consider the example where a homodyne detector is used and show that it is one of the optimal measurement strategies. In section V, we discuss the amplification of CSS using two CSSs that has suffered from linear loss, and finally in section VI we conclude.

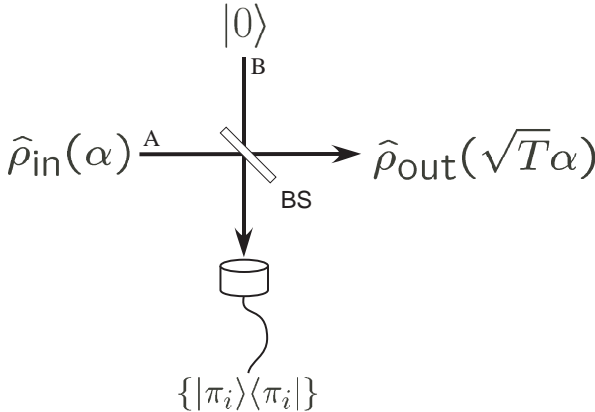


FIG. 1: Schematic of the conditional purification scheme using partial measurement. BS: Beam splitter with transmittivity T .

II. DECOHERENCE OF CSS IN A LOSSY QUANTUM CHANNEL

In this section we briefly summarize the evolution of CSS's under linear dissipation. Let us first define a superposition of two coherent states (CSS) with the amplitudes

$|\pm\beta\rangle$ and the relative phase φ as

$$|\psi_\varphi(\beta)\rangle = \frac{1}{\sqrt{N_\varphi(\beta)}} (|\beta\rangle + e^{i\varphi} |-\beta\rangle), \quad (1)$$

where

$$N_\varphi(\beta) = 2(1 + \cos \varphi e^{-2\beta^2}). \quad (2)$$

We assume β to be real without loss of generality.

In practice, the most dominant loss in optical channels is due to a linear interaction between the signal mode and the vacuum environment. This is modeled by coupling the signal mode to the environment, letting them evolve for some time and finally trace out the states of the environment. A completely positive (CP) map describing such a linear interaction between the signal and the environment is given by [22]

$$\mathcal{L}_L = \exp[-\ln \eta (\mathcal{K}_- - \mathcal{K}_0)], \quad (3)$$

where \mathcal{K}_- and \mathcal{K}_0 are the superoperators defined as

$$\mathcal{K}_- \hat{X} = \hat{a} \hat{X} \hat{a}^\dagger \quad \mathcal{K}_0 \hat{X} = \frac{1}{2} (\hat{a} \hat{a}^\dagger \hat{X} + \hat{X} \hat{a}^\dagger \hat{a}), \quad (4)$$

for an arbitrary operator \hat{X} . The transmission of the environment is denoted by η and thus the linear loss is given by $1 - \eta$. Using the transformation

$$\begin{aligned} \mathcal{L}_L |\alpha_1\rangle\langle\alpha_2| = & \exp \left[-\frac{1}{2}(1-\eta) (|\alpha_1|^2 + |\alpha_2|^2 - 2\alpha_1 \alpha_2^*) \right] \\ & \times |\alpha_1 \sqrt{\eta}\rangle\langle\alpha_2 \sqrt{\eta}|. \end{aligned} \quad (5)$$

we find that the CSS, $\hat{\rho}_{C_\varphi}(\beta) = |\psi_\varphi(\beta)\rangle\langle\psi_\varphi(\beta)|$, under linear dissipation transforms into the mixture

$$\mathcal{L}_L \hat{\rho}_{C_\varphi}(\beta) = p \hat{\rho}_{C_\varphi}(\sqrt{\eta}\beta) + (1-p) \hat{\rho}_0(\sqrt{\eta}\beta), \quad (6)$$

where $\hat{\rho}_0(\sqrt{\eta}\beta)$ is a statistical mixture of coherent states $\hat{\rho}_0(\sqrt{\eta}\beta) = \frac{1}{2} (|\sqrt{\eta}\beta\rangle\langle\sqrt{\eta}\beta| + |-\sqrt{\eta}\beta\rangle\langle-\sqrt{\eta}\beta|)$. Here the fraction of the original state in this mixed state is given by

$$p = \frac{1 + \cos \varphi e^{-2(1-\eta)\beta^2}}{1 + \cos \varphi e^{-2\beta^2}} e^{-2\eta\beta^2}. \quad (7)$$

As expected, the linear lossy interaction with the environment transforms the original pure CSS state into a classical statistical mixture. The aim of this paper is to develop a method by which the decohered state can be probabilistically purified to produce a smaller number of states with higher purity, or in other words; the aim is to increase the value of p .

Finally, we note that the purity defined by $\text{Tr}[\hat{\rho}^2]$ is not a suitable figure of merit for our purpose. One can easily show that, for the mixed CSS in Eq. (6), a smaller amplitude gives a higher purity of the state even for small p . This is because such a state is close to a vacuum state which is completely pure. However, it is obvious that it does not mean the state is close to a pure CSS.

III. PURIFICATION VIA PARTIAL MEASUREMENT

Our proposed scheme for probabilistic purification of CSSs is illustrated in Fig. 1. The state under interrogation is mixed with the vacuum at a beam splitter with the transmission coefficient T . The reflected beam is subsequently measured using a positive operator-valued measure (POVM) generally described by a set of positive operators $\{\hat{\rho}_i\}$ with $\sum_i \hat{\rho}_i = \hat{1}$. Depending on the outcome of this measurement, the transmitted state is probabilistically purified: If the outcomes fall within a certain detection range, the transmitted state is purified, otherwise the state turns out to be worse and is discarded.

Let us first describe the function of the purification scheme when an already pure CSS $\hat{\rho}_{C_\varphi}(\alpha) = |\psi_\varphi(\alpha)\rangle\langle\psi_\varphi(\alpha)|$ is injected into it. In this case, the output of the beam splitter (described by the unitary operator $\hat{B}(T)$) is given by the entangled state

$$\begin{aligned} \hat{B}(T)|\psi_\varphi(\alpha)\rangle_A|0\rangle_B &= \frac{1}{\sqrt{N_\varphi(\alpha)}} \left(|\sqrt{T}\alpha\rangle_A|\sqrt{R}\alpha\rangle_B \right. \\ &\quad \left. + e^{i\varphi}|\sqrt{T}\alpha\rangle_A|-\sqrt{R}\alpha\rangle_B \right), \end{aligned} \quad (8)$$

where $R = 1 - T$ is the reflectivity of the beam splitter. If we now consider only one output and trace out the other, the pure CSS is transformed into a statistical mixture as a result of the coupling to the vacuum environment. The purification protocol now works by making a measurement on the “environmental” mode (mode B) and selecting the outcomes that map $|\psi_\varphi(\alpha)\rangle$ back onto a pure CSS at the output. It implies that the measurement outcomes for successful events have to satisfy

$$\langle\pi_j^s| - \sqrt{R}\alpha\rangle = e^{i\theta_j} \langle\pi_j^s| \sqrt{R}\alpha\rangle, \quad (9)$$

where the superscript s denotes the successful events. The unnormalized conditional output for such outcomes is given by

$$\begin{aligned} &_B\langle\pi_j^s|\hat{B}(T)|\psi_\varphi(\alpha)\rangle_A|0\rangle_B \\ &= \frac{1}{N_\varphi(\alpha)^{1/2}} \langle\pi_j^s| \sqrt{R}\alpha \rangle \left(|\sqrt{T}\alpha\rangle + e^{i(\varphi+\theta_j)}|-\sqrt{T}\alpha\rangle \right) \\ &= \langle\pi_j^s| \sqrt{R}\alpha \rangle \left(\frac{N_{\varphi+\theta_j}(\sqrt{T}\alpha)}{N_\varphi(\alpha)} \right)^{1/2} |\psi_{\varphi+\theta_j}(\sqrt{T}\alpha)\rangle, \end{aligned} \quad (10)$$

The output state of the purifier is therefore a pure CSS with a reduced amplitude and a phase shift with respect to the input state. This means that by applying measurements that fulfill Eq. (9), it is possible to recover the purity of the input CSS.

Let us now consider the purification of a decohered CSS. The input to the purifier is now the mixture

$$\hat{\rho}_{\text{in}}(\alpha) = p_{\text{in}}\hat{\rho}_{C_\varphi}(\alpha) + (1 - p_{\text{in}})\hat{\rho}_0(\alpha). \quad (11)$$

The reflected part of the state is measured using the above mentioned POVM and events corresponding to condition (9) are selected. The resulting density operator of the output state conditioned on this measurement is given by

$$\begin{aligned} \hat{\rho}_{\text{out}}(\sqrt{T}\alpha) &= \frac{p_{\text{in}}P_{C_\varphi}\hat{\rho}_{C_{\varphi+\theta_j}}(\sqrt{T}\alpha) + (1 - p_{\text{in}})P_0\hat{\rho}_0(\sqrt{T}\alpha)}{p_{\text{in}}P_{C_\varphi} + (1 - p_{\text{in}})P_0} \\ &\equiv p_{\text{out}}\hat{\rho}_{C_{\varphi+\theta_j}}(\sqrt{T}\alpha) + (1 - p_{\text{out}})\hat{\rho}_0(\sqrt{T}\alpha) \end{aligned} \quad (12)$$

where

$$\begin{aligned} P_{C_\varphi} &= \text{Tr}_A \left[{}_B\langle\pi_j^s|\hat{B}(T)(\hat{\rho}_{C_\varphi}(\alpha) \otimes |0\rangle\langle 0|)\hat{B}^\dagger(T)|\pi_j^s\rangle_B \right] \\ &= \left| \langle\pi_j^s| \sqrt{R}\alpha \rangle \right|^2 \frac{1 + \cos(\varphi + \theta_j) e^{-2T\alpha^2}}{1 + \cos \varphi e^{-2\alpha^2}} \end{aligned} \quad (13)$$

and

$$\begin{aligned} P_0 &= \text{Tr}_A \left[{}_B\langle\pi_j^s|\hat{B}(T)(\hat{\rho}_0(\alpha) \otimes |0\rangle\langle 0|)\hat{B}^\dagger(T)|\pi_j^s\rangle_B \right] \\ &= \left| \langle\pi_j^s| \sqrt{R}\alpha \rangle \right|^2 \end{aligned} \quad (14)$$

correspond to the probability distributions for detecting the outcomes π_j^s in the states $\hat{\rho}_{C_\varphi}(\alpha)$ and $\hat{\rho}_0(\alpha)$, respectively. As a consequence, one finds the fraction of the CSS after the purification as

$$\begin{aligned} p_{\text{out}} &= \frac{P_{C_\varphi}}{p_{\text{in}}P_{C_\varphi} + (1 - p_{\text{in}})P_0} p_{\text{in}} \\ &= \frac{1}{p_{\text{in}} + P_0/P_{C_\varphi}(1 - p_{\text{in}})} p_{\text{in}}. \end{aligned} \quad (15)$$

The condition for successful purification $p_{\text{out}} > p_{\text{in}}$ is then given by

$$\frac{P_0}{P_{C_\varphi}} = \frac{1 + \cos \varphi e^{-2\alpha^2}}{1 + \cos(\varphi + \theta_j) e^{-2T\alpha^2}} < 1, \quad (16)$$

The maximum purification efficiency is achieved when P_0/P_{C_φ} is minimized. There are two free parameters controlling the magnitude of this fraction, namely θ_j and T . First we note that the phase θ_j is optimized, that is P_0/P_{C_φ} is minimized when $\theta_j = -\varphi$. Second, it is clear that the fraction (16) decreases with decreasing transmissions T . This, on the other hand, means that the amplitude of the CSS is decreasing. Therefore, there is a trade-off between the efficiency of the purification protocol and the amplitude of the purified CSS. Since large amplitude CSSs are desired for many applications, we consider the possibility of amplifying the degraded CSS in Sec. V.

The optimal POVM for the purification protocol is therefore the one that obeys Eq. (9) and simultaneously minimizes the fraction (16) by satisfying the constraint $\theta_j + \varphi = 0$. These conditions provide a nice flexibility to choose among different measurement strategies. Two well known measurement strategies that satisfy the requirements are photon number resolving detectors and

homodyne detectors. If however the photon number resolving detector is used to execute the purification protocol, successful demonstration will only be obtained if the phase between the coherent state components in the CSS, is $\varphi = 0$ or π . Furthermore, these detectors are experimentally very challenging to construct and thus, to date, they are not an integral part of the standard lab.

Fortunately, homodyne detectors (which have matured much further than photon number resolving detectors) also meet the requirements for successful purification. In fact by using homodyne detectors there are no restrictions on the phase φ . In the following section we investigate in greater details the purification of CSS using homodyne detection.

IV. PURIFICATION VIA HOMODYNE MEASUREMENT

A homodyne detector measures a quadrature of the electromagnetic field, with the specific quadratures being determined by the phase, λ , of the intrinsic local oscillator. It is mathematically described by an operator $|x_\lambda\rangle\langle x_\lambda|$ which projects the state onto a continuous set of quadrature eigenstates $\{|x_\lambda\rangle\}$ with λ denoting the quadrature phase. Specific and important examples are the position and momentum eigenstates corresponding to $\lambda = 0$ and $\lambda = \pi/2$, respectively. The probability amplitude associated with the detection of a quadrature eigenvalue, x_λ , from the coherent state $|\beta\rangle$ by homodyne detection is given by

$$\langle x_\lambda | \beta \rangle = \pi^{-1/4} \exp \left[-\frac{1}{2} x_\lambda^2 - \sqrt{2} e^{-i\lambda} x_\lambda \beta - \frac{1}{2} e^{-2i\lambda} \beta^2 - \frac{1}{2} |\beta|^2 \right]. \quad (17)$$

The necessary condition for our purification scheme to work as quoted in Eq. (9) is fulfilled when $\lambda = \pi/2$, that is when the momentum eigenstate is measured. In that case we obtain

$$\langle x_{\pi/2} | -\beta \rangle = e^{i2\sqrt{2}x_{\pi/2}\beta} \langle x_{\pi/2} | \beta \rangle, \quad (18)$$

from which we see that the phase shift introduced by the measurement depends on $x_{\pi/2}$ as

$$\theta = 2\sqrt{2}x_{\pi/2}\beta. \quad (19)$$

Note that the homodyne measurement always allows us to choose the appropriate $x_{\pi/2}$ to optimize θ for any given φ .

In the following we set $k \equiv x_{\pi/2}$. The unnormalized conditional output corresponding to Eq. (10) is then

given by

$$\begin{aligned} {}_B\langle k | \hat{B}(T) | \psi_\varphi \rangle_A | 0 \rangle_B &= \frac{1}{N_\varphi(\alpha)^{1/2}} \langle k | \sqrt{R}\alpha \rangle \left(|\sqrt{T}\alpha\rangle + e^{i(\varphi+\theta)} | -\sqrt{T}\alpha \rangle \right) \\ &= \frac{e^{-\frac{1}{2}k^2 - i\sqrt{2R}\alpha k}}{\pi^{1/4}} \sqrt{\frac{1 + \cos(\varphi + 2\sqrt{2R}\alpha k)e^{-2T\alpha^2}}{1 + \cos \varphi e^{-2\alpha^2}}} \\ &\quad \times \left| \psi_{\varphi+2\sqrt{2R}\alpha k}(\sqrt{T}\alpha) \right\rangle_A, \end{aligned} \quad (20)$$

and one obtains the probability distributions for detecting the $\hat{p}_{C_\varphi}(\alpha)$ and $\hat{p}_0(\alpha)$ as

$$P_{C_\varphi}(k) = \frac{e^{-k^2}}{\pi^{1/2}} \frac{1 + \cos(\varphi + 2\sqrt{2R}\alpha k)e^{-2T\alpha^2}}{1 + \cos \varphi e^{-2\alpha^2}} \quad (21)$$

and

$$P_0(k) = \frac{e^{-k^2}}{\pi^{1/2}}, \quad (22)$$

respectively.

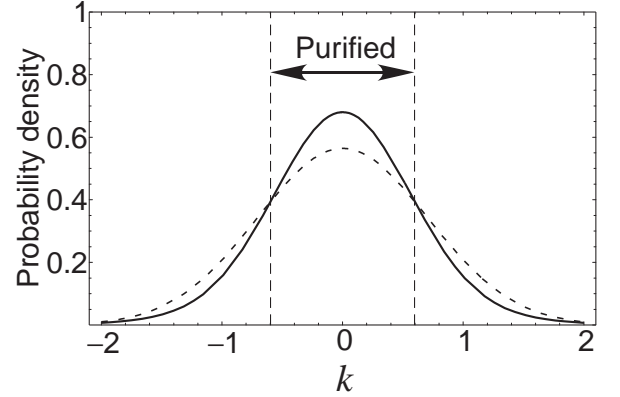


FIG. 2: Probability quadrature distributions of a CSS P_{C_0} with $\varphi = 0$ (solid line) and a mixture of coherent states P_0 (dotted line). $T = 0.5$ and $\alpha = 1$. The purification protocol is successful when the measurement outcome falls within the interval indicated by the dashed vertical lines.

Figs. 2 and 3 show these probability distributions for $\varphi = 0$ and π , respectively. The probability distributions P_0 , which is represented by the dashed curves, are Gaussian, while the probability distributions for the CSS, P_{C_φ} , (represented by solid lines) are non-Gaussian due to the quantum coherence between the two coherent state components. As discussed above, these distinct differences between the probability distributions enable the purification protocol: It succeeds when the absolute quadrature value falls within a certain threshold for $\varphi = 0$ and outside a certain threshold for $\varphi = \pi/2$, since in these regions the probability for a CSS to occur is larger than

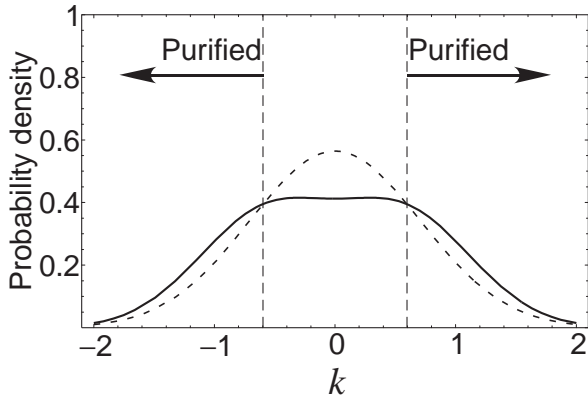


FIG. 3: Probability quadrature distributions for a CSS P_{C_φ} with $\varphi = \pi$ (solid line) and a mixture of coherent states P_0 (dotted line). $T = 0.5$ and $\alpha = 1$. The purification protocol is successful when the measurement outcome falls outside the interval indicated by the dashed vertical lines.

the probability for $\hat{\rho}_0(\alpha)$ to occur. The efficiencies of the purification protocol for $\varphi = 0$ and $\varphi = \pi$ are illustrated in Figs. 4 and 5, respectively. In case of $\varphi = 0$, the purification condition of Eq. (9) is satisfied in the range given by $|\cos \theta| > e^{-2R\alpha^2}$ and the efficiency of the purification protocol is optimised for $\theta = 0$. The protocol works more efficiently when the initial CSS has the phase $\varphi = \pi$. In that case, purification is achieved in the range given by $|\cos \theta| < e^{-2R\alpha^2}$ and is maximized at $\theta = \pi$ where the initial input phase $\varphi = \pi$ is transformed into $\varphi = 0$ after purification. The maximum increase of p_{out} as a function of p_{in} for $T = 1/2$ and $\alpha = 1$ is depicted in Fig. 6, and we see that the improvement for these parameters is highest around $p_{\text{in}} = 1/2$.

In Figs. 7 and 8, we show how the purification efficiency depends on the amplitude α and the transmittance of the beam splitter T , respectively, for an input state with $p_{\text{in}} = 0.5$. From Fig. 7, we see that the purification of states with $\varphi = 0$ (represented by the solid curve) is most effective around $\alpha \sim 1$ whereas for states with $\varphi = \pi$ the efficiency increases with smaller amplitudes. In Fig. 8, where the purification efficiency is plotted versus the transmission coefficient, it is evident that small transmission coefficients are advantageous. However, as already pointed out above, small transmission coefficients are on the other hand not desirable since it degrades the amplitude of the state. Note that, obviously the purification does not work at $T = 1$. Although, in Fig. 8, $p_{\text{out}}/p_{\text{in}}$ is still larger than 1 for $\varphi = \pi$ at $T = 1$, the probability amplitude $P_{C_{\pi/2}}(0)$ goes to zero and thus this event never happens. These results, therefore, show that our scheme can be used to purify small amplitude CSSs, which are exactly the ones that recently has been produced [10]. However, the reduction of amplitude of the CSS is unavoidable in our scheme and it is therefore desirable to amplify the amplitude of the CSSs after

purification. This is the topic of the next section.

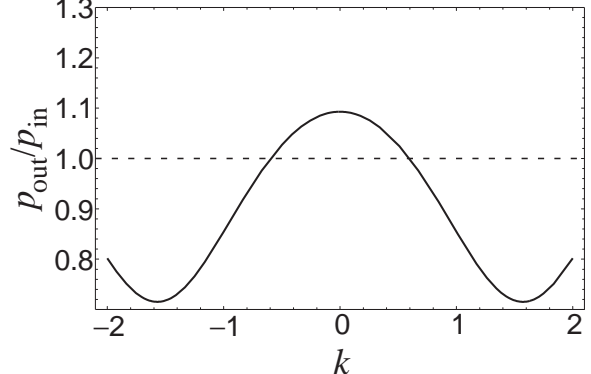


FIG. 4: Purification efficiency for the CSS with $\varphi = 0$ conditioned on the homodyne detection outcomes. The phase of the local oscillator is chosen to measure the quadrature $k \equiv x_{\pi/2}$. $T = 0.5$, $\alpha = 1$, and $p_{\text{in}} = 0.5$.

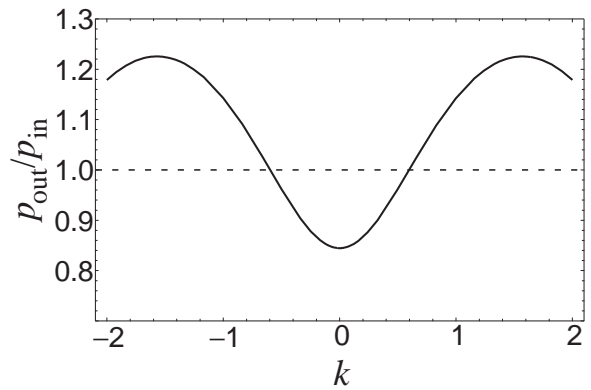


FIG. 5: Purification efficiency for the CSS with $\varphi = \pi$ conditioned on the homodyne detection outcomes. The phase of the local oscillator is chosen to measure the quadrature $k \equiv x_{\pi/2}$. $T = 0.5$, $\alpha = 1$, and $p_{\text{in}} = 0.5$.

V. AMPLIFICATION OF COHERENT SUPERPOSITION STATES

Lund *et al.* have proposed a scheme to conditionally produce a large amplitude CSS from two small amplitude CSSs by using two 50/50 beam splitters, an ancillary coherent state and two on/off photon detectors [11], and later on the scalability of this scheme was studied in details [12]. They pointed out that when one uses a weakly squeezed single photon state corresponding to a small CSS (which in practice inevitably consists of a mixture between the single photon state and a vacuum state) it is possible to reduce the squeezed vacuum component during the amplification process. In this section, we discuss

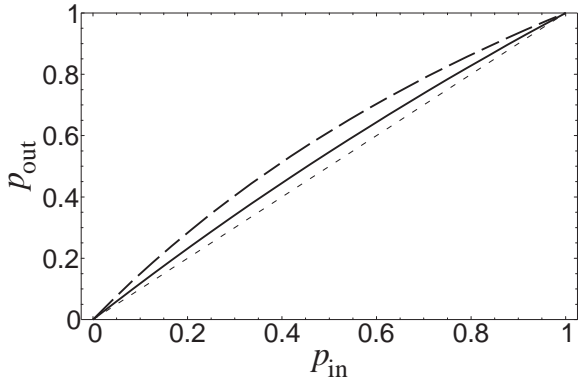


FIG. 6: Dependence of the p_{out} on p_{in} for the CSS with $\varphi = 0$ (solid line) and $\varphi = \pi$ (dashed line) where the outputs are conditioned on the measurement outcomes $k = 0$ and $k = \pi/2$, respectively. $T = 0.5$ and $\alpha = 1$. The dotted line denotes $p_{\text{out}} = p_{\text{in}}$ as a reference.

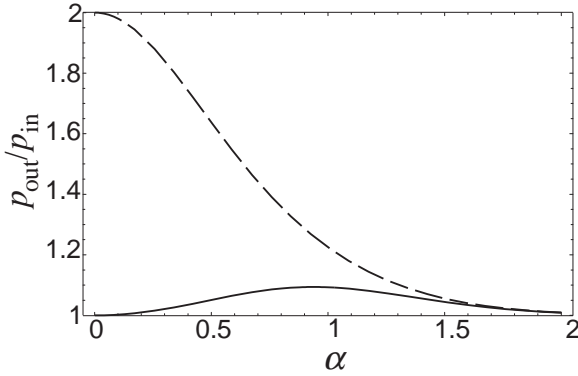


FIG. 7: Dependence of the purification gain on the initial amplitude for CSSs with $\varphi = 0$ (solid line) and $\varphi = \pi$ (dashed line). $T = 0.5$ and $p = 0.5$. The measurement outcome is selected to satisfy the optimal condition $\varphi + \theta = 0$.

the application of such a scheme to obtain a larger amplitude CSS from two decohered CSSs. We show that, the decoherence is, unfortunately, in most cases increased as a result of the amplification process.

The scheme proposed in Ref. [11] is illustrated in Fig. 9. Two copies of the CSSs with small amplitude are combined on a 50/50 beam splitter. Then one of the outputs is mixed with a coherent state with amplitude $\sqrt{2}\alpha$ on a 50/50 beam splitter. Subsequently the two outputs are measured using two on/off photon detectors. If both detectors click, the remaining quantum state is projected onto a larger CSS. In addition to the amplification of the amplitude, the projection process also filter out the squeezed vacuum component when the inputs are two mixed states of weakly squeezed single photon and vacuum.

Now, suppose that the input is two copies of the decohered CSS $\hat{\rho}_{\text{in}}(\alpha)$ defined in Eq. (11). Then, the input

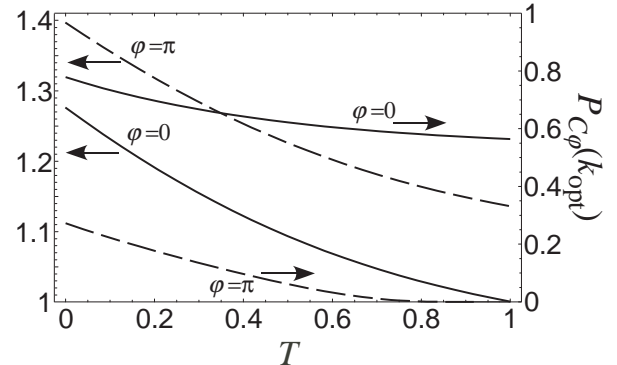


FIG. 8: Dependence of the purification gain on the transmittance of the tapping beam splitter T for a plus cat state ($\varphi = 0$, solid line) and a minus cat state ($\varphi = \pi$, dashed line), under condition of $p = 0.5$, $\alpha = 1$. The value of k is selected to satisfy the condition $\varphi + \theta = 0$.

state is described by the tensor product

$$\begin{aligned} \hat{\rho}_{\text{in}} \otimes \hat{\rho}_{\text{in}} = & p_{\text{in}}^2 \hat{\rho}_{C\varphi} \otimes \hat{\rho}_{C\varphi} + (1 - p_{\text{in}})^2 \hat{\rho}_0 \otimes \hat{\rho}_0 \\ & + p_{\text{in}}(1 - p_{\text{in}}) (\hat{\rho}_{C\varphi} \otimes \hat{\rho}_0 + \hat{\rho}_{C\varphi} \otimes \hat{\rho}_0), \end{aligned} \quad (23)$$

and in the conditioned amplified output state, only the first term is mapped onto a large CSS whereas all other terms are transformed into a mixture of coherent states. As a result, the fraction of a CSS in the conditioned output states are approximately degraded as $p_{\text{out}} \sim p_{\text{in}}^2$. More precisely, the output probabilities p_{out}^+ and p_{out}^- with inputs $\hat{\rho}_{C_0}(\alpha)$ and $\hat{\rho}_{C_\pi}(\alpha)$, respectively, are given by

$$p_{\text{out}}^\pm = \frac{\frac{1+e^{-4\alpha^2}}{(1\pm e^{-2\alpha^2})^2} p_{\text{in}}^2}{\frac{1+e^{-4\alpha^2}}{(1\pm e^{-2\alpha^2})^2} p_{\text{in}}^2 + \frac{2p_{\text{in}}(1-p_{\text{in}})}{1\pm e^{-2\alpha^2}} + (1-p_{\text{in}})^2}. \quad (24)$$

Note that the conditioned output CSS with the probability p_{out}^\pm is always $|\psi_{C_0}(\sqrt{2}\alpha)\rangle$ [11]. The parameter region where the inputs are purified during the conditional process can be evaluated from the condition $p_{\text{out}}^\pm > p_{\text{in}}$. First, we find that if the phase φ is 0 (that is $\hat{\rho}_{C_0}(\alpha)$ is amplified), the inequality cannot be satisfied. Therefore, in this case, the output probability p_{out}^+ is always smaller than the input probability, or in other words, the decoherence is always amplified. However, if the amplitude of decohered CSS with $\varphi = \pi$ (that is $\hat{\rho}_{C_\pi}(\alpha)$) are amplified, then the inequality $p_{\text{out}}^- > p_{\text{in}}$ can be satisfied if

$$p_{\text{in}} > \frac{1}{2} (e^{2\alpha^2} - 1)^2. \quad (25)$$

This implies that the average photon number of the input CSS must be $\alpha^2 < \ln(\sqrt{2} + 1)/2 \approx 0.44$ for successful amplification of the amplitude without amplifying the decoherence.

Finally, we investigate the possibility to repeat the purification process by concatenating this amplification scheme. The situation considered here is illustrated in Fig. 10. Two initial states $\hat{\rho}_{\text{in}}(\alpha)$ are purified in parallel by the purification processes with $T = 1/2$. Once the purified outputs $\hat{\rho}_{\text{out}}(\alpha/\sqrt{2})$ from both processes are simultaneously obtained, the outputs are injected into the amplification process to obtain the final output which has the original amplitude α . Let us now determine whether the output probability p_{out} is larger than the input probability p_{in} for such a machine: Since the phase of the CSS obtained from the amplification process is always $\varphi = 0$, we assume the initial states to have $\varphi = 0$. We then look for parameters where $p_{\text{out}} > p_{\text{in}}$ by replacing p_{in} in Eq. (24) by $p_{\text{in}}/(p_{\text{in}} + P_0/P_{C_\varphi}(1 - p_{\text{in}}))$ (which is the output probability from the purification step). However, unfortunately, a parameter interval fulfilling such criterion does not exist, and we conclude that for all possible amplitudes α , the decoherence is amplified along with the amplitudes. It suggests that when the goal is to generate large amplitude CSSs from smaller ones by using the conditional processes with linear optics proposed in Ref. [11], we have to be careful about the effects of linear loss even if the initial states contain only a very small fractions of mixtures of coherent states. As we have shown, the decoherence is in most cases amplified during the conditional generation of large CSSs.

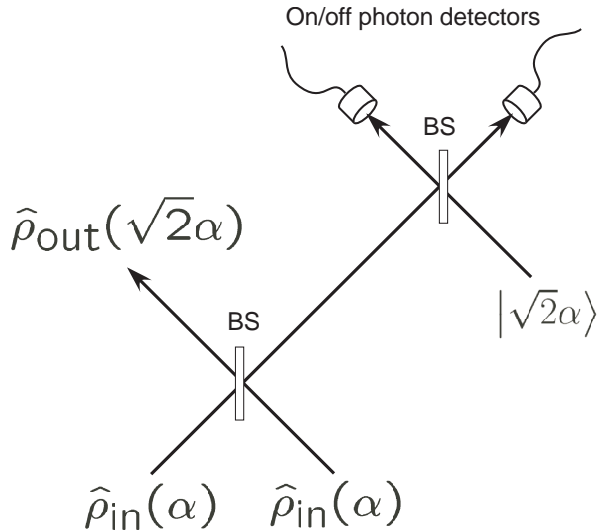


FIG. 9: A schematic of the CSS-amplification process [11] with the decohered input and output.

VI. CONCLUSIONS

In this paper, we have investigated a simple scheme to recover the quantum coherence of decohered coherent

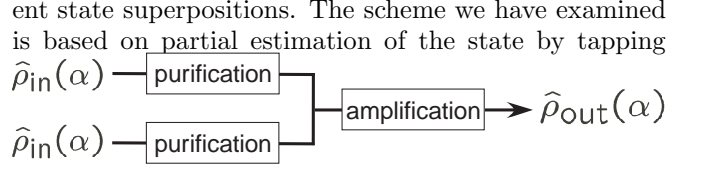


FIG. 10: Concatenation of the purification and amplification processes.

off a part of it using a beam splitter, measuring the reflected part by homodyne detection and finally select out favourable events that maps the decohered state onto a purer state.

We derived the condition for the measurement to maximize the efficiency of the purification and showed that homodyne measurement is one of the optimal strategies. Since homodyne measurement is a well developed technique, our purification scheme is experimentally easier to implement than previously proposed purification protocols. We therefore believe that our scheme can be directly implemented in current on-going experiments on the generation of CSS to compensate for losses and increase the nonclassicality of the states.

In addition, we showed that this simple measurement-induced scheme inevitably causes further amplitude degradation and is not suitable for the purification of large amplitude CSS with $\alpha \geq 2$. Moreover, we have discussed the possibility to restore the degraded amplitude by the linear optical scheme proposed in [11]. If the initial CSSs are decohered due to a linear loss, the scheme is increasing not only the amplitude but also the degree of the mixture. We showed that, even combining this scheme with the purification process, it is still hardly possible to recover the coherence of CSS. Note that, also in the context of entanglement purification, it has been suggested in [18] that the purification of entangled coherent states decohered by linear loss also seems to be difficult by using only linear optics and photon counting without ancillary CSSs. These results emphasize the importance of the further investigations of the purification scheme.

Acknowledgments

ULA acknowledges the financial support from the EU project COVAQIAL (FP6-511004).

[1] V. Giovannetti, S. Guha, S. Lloyd, L. Maccone, J. H. Shapiro, and H. P. Yuen, Phys. Rev. Lett. **92**, 027902 (2004).

[2] A. S. Holevo, Tamagawa University Research Review, **4**, 1 (1998); extended version, quant-ph/9809023.

[3] H. Yonezawa, T. Aoki, and A. Furusawa, Nature (London) **431**, 430 (2004).

[4] S. L. Braunstein and A. K. Pati eds., *Quantum Information with Continuous Variables*, (Kluwer 2001).

[5] S. Lloyd and S. L. Braunstein, Phys. Rev. Lett. **82**, 1784 (1999).

[6] D. Gottesman, A. Kitaev, and J. Preskill, Phys. Rev. A **64**, 012310 (2001).

[7] S. D. Bartlett and B. C. Sanders, Phys. Rev. A **65**, 042304 (2002).

[8] M. Sasaki, K. Wakui, J. Mizuno, M. Fujiwara, and M. Akiba, in *Quantum Communication, Measurement and Computing*, (eds. S. M. Barnett *et al.* AIP, New York, 2004) 44.

[9] M. Dakna, T. Anhut, T. Opatrný, L. Knöll, and D.-G. Welsch, Phys. Rev. A **55**, 3184 (1997).

[10] J. Wenger, R. Tualle-Brouri, and P. Grangier, Phys. Rev. Lett. **92**, 153601 (2004).

[11] A. P. Lund, H. Jeong, T. C. Ralph, and M. S. Kim, Phys. Rev. A **70** 020101(R) (2004).

[12] H. Jeong, A. P. Lund, and T. C. Ralph, Phys. Rev. A **72** 013801 (2005).

[13] S. J. van Enk and O. Hirota, Phys. Rev. A **64**, 022313 (2001).

[14] H. Jeong, M. S. Kim, and J. Lee, Phys. Rev. A **64**, 052308 (2001).

[15] H. Jeong and M. S. Kim, Phys. Rev. A **65**, 042305 (2002).

[16] T. C. Ralph, W. J. Munro, and G. J. Milburn, Proc. SPIE **4917**, 1 (2002); quant-ph/0110115.

[17] T. C. Ralph, A. Gilchrist, G. J. Milburn, W. J. Munro, and S. Glancy, Phys. Rev. A **68**, 042319 (2003).

[18] H. Jeong and M. S. Kim, Quantum Inf. Compt. **2**, 205 (2002).

[19] J. Clausen, L. Knöll, and D. -G. Welsch, Phys. Rev. A **66**, 062303 (2002).

[20] P. T. Cochrane, G. J. Milburn, and W. J. Munro, Phys. Rev. A **59**, 2631 (1999).

[21] S. Glancy, H. M. Vasconcelos, and T. C. Ralph, Phys. Rev. A **70**, 022317 (2004).

[22] D. F. Walls and G. J. Milburn, *Quantum Optics* (Springer-Verlag, Berlin, 1994).